THE JOURNAL OF PHYSICAL CHEMISTRY C

Article

pubs.acs.org/JPCC

Time-Resolved Nanosecond Imaging of Nanoscale Condensed Phase Reaction

Garth C. Egan, Thomas LaGrange,[‡,§] and Michael R. Zachariah*

Department of Chemical and Biomolecular Engineering and Department of Chemistry and Biochemistry, University of Maryland, College Park, Maryland, 20742, United States

[‡]Physical and Life Sciences Directorate, Lawrence Livermore National Laboratory, 7000 East Avenue, Livermore, California 94550, United States

Supporting Information

ABSTRACT: The reaction between metallic fuel and oxygen carriers produced by the laser heating of aluminum and copper oxide (CuO) nanoparticles (NPs) was investigated (NPs) using movie mode dynamic transmission electron microscopy (MM-DTEM), which enables multiframe imaging with nanometer spatial and nanosecond temporal resolution. Nanothermite materials heated *in situ* at ~10^{11} K/s showed significant morphological changes on time scales of 1−5 μs. The resulting structures were typically phase-separated into adjoining spheroids. Further analysis with energy dispersive spectroscopy (EDS) and selected area electron diffraction (SAED) was used to determine the extent of reaction. Bulk scale reaction experiments using temperature jump wire heating (~10^5K/s) revealed that both the reaction products and general processes were comparable to the reactions driven by the DTEM laser heating. These results indicate that condensed phase and interfacial reactions are fast and dominant mechanisms in nanothermite combustion.

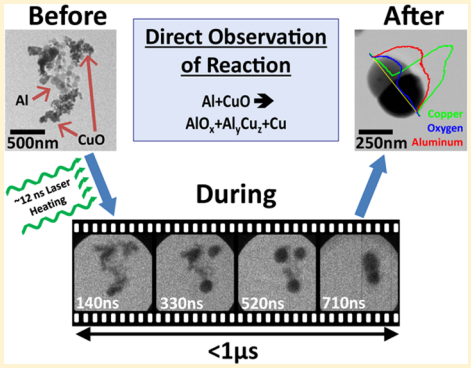

INTRODUCTION

Energetic mixtures made from metal fuel (e.g., Al, B, Si, Mg) and metal oxide oxidizer (e.g., CuO, Fe_2O_3, Bi_2O_3, MoO_3) nanoparticles are known as nanothermites or metastable intermolecular composites (MICs) and have many commercial and research applications due to their high energy density, relatively low gas release, and fast reaction rates.[1,2] Recent research efforts have focused on developing high performance systems with higher burn rates as well as more controllable heat release, though optimization of nanothermite systems requires a better understanding of the combustion mechanisms and the times scales of the salient processes. Combustion dynamics are primarily influenced by the mode of heat transfer and the reaction pathway. Heat transfer occurs through a number of mechanisms (e.g., conduction, convection, radiation, and/or advection[3−6]) and reaction as well can proceed through many different mechanisms such as heterogeneous gas-condensed phase (burning particles in oxygen),[7,8] interfacial condensed phase (oxygen transfer across a boundary between two molten or solid materials),[9−11] or more complex material response.[5,12,13] The gas phase reaction pathway occurs by the reduction of the metal oxide (e.g., $Fe_2O_3 \rightarrow Fe_3O_4$, $CuO \rightarrow Cu_2O$, $Co_3O_4 \rightarrow CoO$), which releases gaseous oxygen,[7] thus allowing the Al-NP fuel to burn ($Al \rightarrow Al_2O_3$) in a high pressure oxidizing environment. Alternatively, condensed phase reactions occur by the diffusion of oxygen through solid and molten phases of these materials across their shared interfaces. In such reactions, the initial energy release drives sintering and coalescence, which creates larger interfaces and drives reaction faster (a process dubbed reactive sintering).[9] Lastly, a more complex response has been proposed, which involves the spallation of the aluminum from pressure build up within its native oxide shell.[5,12,13]

Some insight about the mechanisms involved in these processes has been gained through controlled "bulk" reaction experiments, though these results are difficult to interpret due to the multiphase, rapidly evolving, nonequilibrium propagation of the reaction. The potential effects of different mechanisms often overlap, leading to varying interpretations of the results and contradicting theories.[13,14] Our lack of knowledge of the underlying mechanisms stems from the difficulty to experimentally observe the nanoscale changes occurring in these materials on the relevant time scales associated with the rapid heating rates and high temperatures intrinsic to the reaction and combustion dynamics. The dynamic transmission electron microscope (DTEM) at Lawrence Livermore National Laboratory (LLNL) enables the direct observation of morphological changes in nanothermites under very rapid heating conditions which can exceed 10^{11} K/s.[15−18] This allows us to isolate and probe the fundamental mechanisms and unit processes of combustion in nanothermites. Laser heating effectively enables instantaneous heating relative to typical

Received: August 21, 2014
Revised: December 9, 2014
Published: December 17, 2014

DOI: 10.1021/jp5084746
J. Phys. Chem. C 2015, 119, 2792−2797

reaction rates and heat losses. Further, these experiments occur in vacuum, which prevents any significant heterogeneous gas-condensed phase reaction. Thus, such an experiment can capture the interfacial condensed phase interaction of these nanoparticle systems, without the convoluting effects of gas phase chemistry and heat transfer to and from the environment.

With this approach we can garner information about the underlying properties of the condensed phase mechanism, which in turn allows us to determine what role it plays in the bulk combustion of nanothermites with the key factors being the chemistry, the time scales of the reactions, and the overall physical response of the system. Proper determination of the chemical reaction involved will allow us to understand if this mechanism can be responsible for generating enough energy to drive self-sustaining combustion. Directly measuring the time scales associated with microstructural change and reaction will also allow us to differentiate between mechanisms controlling the flame prorogation rate. For instance, if the condensed phase reaction is significantly faster than the bulk response it follows that heat transfer rather than chemical reaction rate is the limiting factor in flame propagation rate. Lastly for the physical response, we can determine if any complex behavior such as the spallation of the molten metal fuel occurs.[12,13] Furthermore, if the physics observed through DTEM are occurring during bulk reaction, the products of both classes of experiments must be consistent.

EXPERIMENTAL SECTION

Al/CuO was chosen as a test system because of its wide use and the large number of studies pertaining to these materials. The aluminum nanoparticles purchased from Novacentrix were spherical having a nominal particle size of 80 nm. The CuO was obtained from Sigma-Aldrich and had a primary particle size of <50 nm. Samples were prepared by adding Al with roughly three times the amount of CuO to ethanol, ultrasonicating for ~5 min, and then dispersing the suspension onto TEM grids.

We used a DTEM which has been recently modified to allow multiframe acquisition (movie mode DTEM or MM-DTEM) over large temporal ranges from a few nanoseconds to hundreds of microseconds. The details of this instrument can be found in previous articles.[15−18] In short, MM-DTEM is equipped with a pulse shaping laser and a high-speed deflector system. The pulse shaping laser produces a series of ultraviolet laser pulses with user-defined pulse durations and delays that produces a defined electron pulse train via linear UV photoemission. Each pulse captures an image of the sample at a specific time. The high-speed electrostatic deflector located below the sample directs each pulse (image) to a separate patch on a large, high-resolution CCD camera. At the end of the experiment, the entire CCD image is read out and segmented into a time-ordered series of images, i.e., a movie. The current technology produces 9-frame movies and for these studies, we used 20 and 50 ns electron pulse durations and delays between pulses of 95 and 550 ns.

The TEM specimens were flash heated by a second laser (1/e^2 diameter of 135 μm) operating at a wavelength of 532 nm and a pulse duration of 12 ns to initiate the reaction between the Al nanoparticle fuel and CuO oxidizer nanoparticles. Stochastic electron−electron scattering events within the high intensity electron imaging pulses cause a reduction in spatial resolution of movie mode. The DTEM can also function in a traditional thermionic emission mode (i.e., continuous wave (CW) mode) to obtain higher spatial resolution images of prereaction and post-mortem microstructure to observe in more detail the initial structure and final morphological changes after the specimen has cooled to ambient temperatures. Further analysis on the samples heated in the DTEM was performed using another TEM (JEOL JEM 2100F) with scanning and energy dispersive X-ray spectroscopy (EDS) capabilities, and the crystalline structure was analyzed with selected area diffraction (SAD). Additionally, bulk combustion experiments were performed using a temperature jump (T-jump) wire heating setup at heating rates of ~5 × 10^5 K/s. The experiments were done in air and in a time-of-flight mass spectrometer with ~100 μs resolution.[7,19,20]

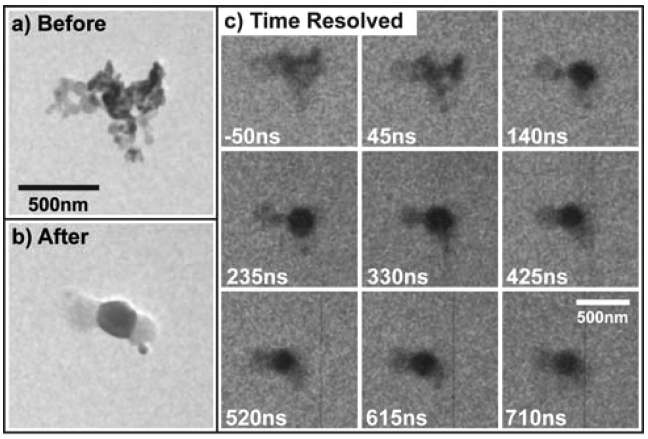

Figure 1. Morphological changes of Al and CuO NPs heated with a 532 nm laser (Pulse length= 12 ns; Peak laser fluence =0.3 kJ/m^2). Images a and b were taken in conventional TEM thermionic mode and the images of part c were taken with pulsed electrons. (a) Aggregate prior to heating. (b) Resulting reacted material morphology. (c) MovieMode DTEM image sequence showing the change in morphology with time. Each frame was taken with a ~20 ns electron pulse duration and 95 ns time delay between pulses. The listed times are relative to the peak intensity of the ~12 ns sample heating laser pulse. The same scale is used for both images a and b with another scale shared by all the images of part c.

RESULTS AND DISCUSSION

Figure 1 shows an example of a small (~500 nm) aggregate that, under rapid heating, reacted and evolved within a period of 600 ns. Figure 1a shows a thermionic mode image of the aggregate prior to heating. The aluminum particles, being a low atomic number material, are weakly contrasted in the image, spherically shaped (left side of the aggregate), and easy to distinguish from the darker more irregularly shaped CuO particles (central region of the aggregate). Figure 1b shows a thermionic mode image of the resulting morphology after heating the aggregate with a 0.3 kJ/m^2 laser pulse. The original nanostructured morphology has been lost, having transitioned from <50 particles into 3 larger, phase-separated regions. Being denser, the copper-rich center region appears darker, while the two surrounding lighter areas are aluminum rich with a morphology that partially resembles the initial configuration of the aggregate. Figure 1c shows a series of time-resolved images taken with the movie mode pulsed electrons. Morphological changes are observed to initiate within 45 ns of the laser heating pulse. Within 235 ns, the central CuO region was fully molten and spherical in shape, while Al particles can be discerned as distinct shapes, even with the low signal-to-noise ratio. By 425 ns, the Al-NPs coalesced toward the CuO region, losing their

DOI: 10.1021/jp5084746
J. Phys. Chem. C 2015, 119, 2792−2797

initial nanostructured character and reducing their specific surface area. At 615 ns, the morphology of the reacted aggregate is similar to that of Figure 1b, and no further significant changes in overall structure were observed. While further chemistry or morphological changes that are beyond the limited spatial resolution may have occurred past this time, such behavior is assumed to be negligible in regards to the overall reaction process. This assumption stems from the fact that anything other than minimal reaction or evolution of the structure would be associated with high temperatures, which would drive further coalescence that could be observed with the resolution of the pulsed electron images.

Through repeated experimentation with many different aggregates, the general characteristics of the microstructural evolution shown in Figure 1 were consistently observed. That includes the product morphologies always being phase separated into distinct regions and the most significant observable morphological change starting in the CuO regions with first melting and then coalescence. Under conventional, slow-rate heating, Al particles, having a melting point of 933 K, melt before CuO, which has a much higher melting point of ~1600 K. However, the laser pulse heated nanoparticles behave differently. Al nanoparticles have a 3 nm thick native oxide (mp = 2345 K) shell, which delays the onset of particle coalescence to above 1300 K.[21] Second, as verified by calculations using the Mie solution to Maxwell's equations for 75 nm diameter particles, a CuO particle absorbs ~3 times more energy of 532 nm light than an Al particle.[22,23] Thus, being hotter, CuO particles are expected to melt first under laser heating.

While the general morphological progression was consistent between experiments, time scales of the observed behavior were significantly affected by aggregate size and morphology. For example, in Figure 1 few significant changes were observed after ~600 ns in these small aggregates, but larger aggregates were observed to evolve over much longer periods of ~6 μs. Likewise, the observed onset of melting in large CuO particle regions was delayed significantly, e.g., for the case shown in Figure 2, no discernible morphological changes were observed until 4.3 μs after the laser heating pulse. Conversely, small CuO aggregates (<500 nm) melted fast (within ~100 ns). In comparison to these time scales, melting should be instantaneous (on the order of the 12 ns laser heating pulse), which suggests that the CuO was not yet hot enough to melt, and the observed melting at longer delays occurred by heat released from reaction and/or due to a reduced melting temperature from alloying and/or oxide reduction.

The initial energy deposition from the laser heating pulse occurs within 12 ns, thus any additional heating occurring within this delay results from the exothermic reaction of Al and CuO. In the case where exothermic reaction raises the material to the melting point, the delay is an approximate measure of the diffusion rate of oxygen across the interface between the two materials. Such behavior could be accompanied by local morphological changes too small to be resolved in the pulsed electron images. Additionally, with no possible exothermic reaction, pure CuO heated by the same laser pulses would either melt instantaneously, i.e., within the pulse duration of the heating laser, or not at all. However, experiments using only CuO-NPs contradict this expectation. Indeed, size dependent delays did occur in a manner that was qualitatively similar to the Al-CuO samples (an example of this can be found Figure S1 of the Supporting Information). In this case, the material was at its peak temperature immediately following the irradiation by sample drive laser pulse, and thus we ascribe the delay in melting to oxide reduction, as CuO nanoparticles, upon sufficient heating in vacuum, reduce to Cu_2O, and eventually to Cu, both of which have lower melting points than CuO.[24] To test that this chemical evolution occurred within the TEM vacuum conditions used in these experiments, selected area diffraction (SAD) patterns were taken for the laser heated CuO. From these observations, the presence of Cu_2O and Cu in the products was confirmed (see Supporting Information for more detail), indicating that laser heating alone was sufficient to cause reduction, which likely triggered the melting.

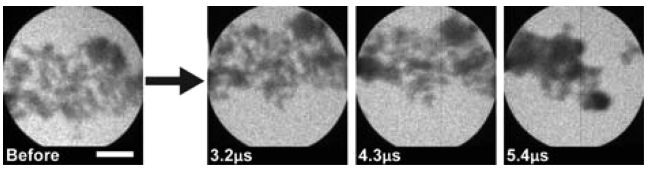

Figure 2. Morphological change of an Al-CuO aggregate that was significantly delayed (heating laser pulse length = 12 ns; peak laser fluence = 0.3 kJ/m^2). No discernible changes were observed until 4.3 μs. All images were taken with ~50 ns electron pulses with 550 ns delays between images. The scale is the same for all images with the scale bar representing 500 nm.

Assuming that the observed delay is associated with the time scale for oxide reduction, the size dependence may derive from temperature rise from laser light absorption being less for the large aggregates. Given the dense packing of the CuO-NPs, the particles on the upper layers of the aggregate scattered and absorbed much of the impinging laser light, and thus the particles in the deeper layers of the aggregate absorbed less energy, which reduced the average, equilibrated aggregate temperature. As a point of comparison, from Mie scattering calculations, as CuO particle size increases above 175 nm, the absorption efficiency per volume decreases with diameter.[22,23] Thus, the larger, dense aggregates will have a lower average temperature, and therefore slower reduction kinetics, which can increase the length of the delay. Associated kinetics can be better understood by modeling the laser heating, but unfortunately light absorption by the NP aggregates is very complex, and nanometer differences in shapes can lead to ~1000 K differences in modeled temperature, thus providing large uncertainties.[21]

The characteristic diffusion time is defined as $\tau = l^2/D$, where l is the characteristic length scale and D is the diffusion coefficient. The important length scale here is the primary particle size radius. For a 30 nm diameter particle, the observed delays of 500 ns and 5 μs correspond to effective diffusivities of $\sim 4.5 \times 10^{-6}$ and $\sim 4.5 \times 10^{-7}$ cm^2/s, respectively. While these values are high compared to the reported oxygen diffusivities in copper oxide ($\sim 10^{-9}$ cm^2/s for O in Cu_2O at ~1500 K),[25] at high temperatures and under vacuum conditions, CuO is far outside of equilibrium stability.[24] If we assume an activation energy of ~1−2 eV (typical values found for copper oxide)[19,26] for diffusion, the difference in estimated diffusivities can be accounted by a ~200−350 K difference in temperature between the two cases, which is consistent with the absorption and temperature estimates described above.

This explanation implies that exothermic reaction was not necessary to promote the morphological changes observed in these experiments. To evaluate this further, elemental analysis was performed using energy dispersive X-ray spectroscopy

DOI: 10.1021/jp5084746
J. Phys. Chem. C 2015, 119, 2792−2797

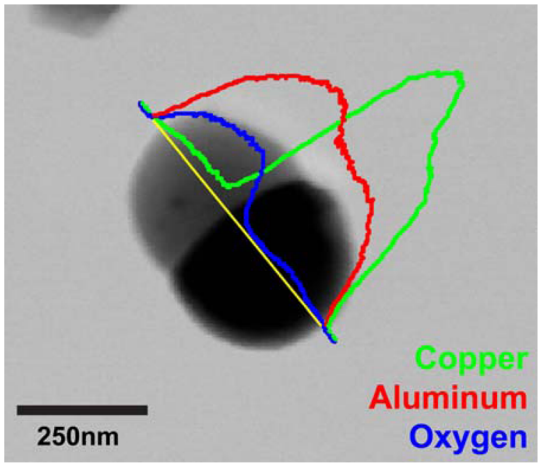

Figure 3. Postreaction product from an Al/CuO laser heating experiment that was analyzed with an EDS line scan. The red line indicates the intensity of the Al signal, green represents Cu, and blue represents O. The results indicate a lighter Al/O phase and a darker Cu/Al phase.

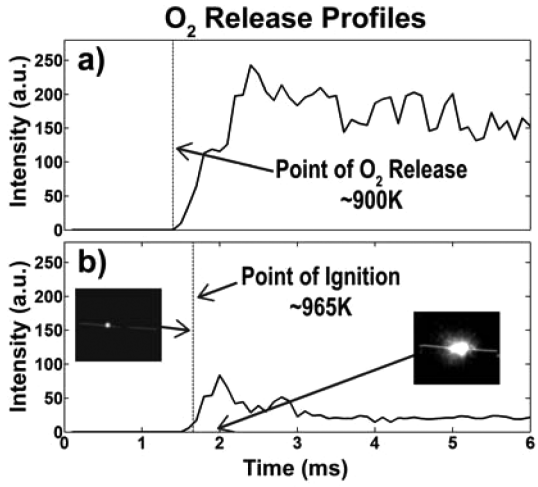

Figure 4. O_2 temporal evolution from *T*-jump mass spectrometry in arbitrary units (a.u.) of intensity of (a) CuO and (b) Al/CuO. Samples were heated at ~3.5 × 10^5 K/s on a platinum wire and the temperature was calculated from the wire resistance. The temperatures listed are the average of several runs and the point of ignition was measured with a high speed video camera, frames of which are inset on part b. From the plot we note that CuO particles first released oxygen at temperatures below ignition followed by a rapid release of O_2 during combustion. Note that the fluctuation in signal intensity can be attributed to measurement noise.

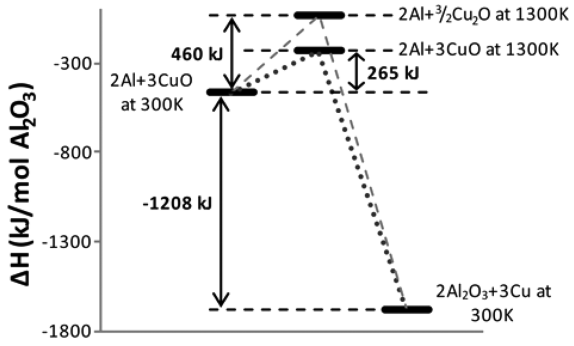

Figure 5. Energy diagram for the system. The elevated states represent the reactants heated to 1300 K. At the highest level, 3CuO has also decomposed to $^3/_2Cu_2O + {}^3/_4O_2$. In both cases the energy needed to reach that point is only 22−38% of the total energy released from reaction.

(EDS) line scans as in Figure 3. These results clearly confirm that the light areas are Al rich and the darker areas are Cu rich. Further they indicate that the aluminum was significantly oxidized. In addition there appears to have been some alloying between the Al and Cu, which confirms that there was significant interaction between the Al and CuO, including the exchange of oxygen for reaction. However, it should be noted that the total amount of oxygen is diminished in comparison to the amount of Cu present. This loss of oxygen is consistent with an initial reduction to Cu_2O, which led to both coalescence and subsequent reaction.

Though laser heating was nonuniform due to compositionally driven variation in the optical absorption, the DTEM experiments compared well with reaction dynamics observed in nanocomposite thermally driven at lower rates. Figure 4 shows results from *T*-jump experiments where CuO−NPs and Al/CuO nanothermites were coated on a 76 μm diameter Pt wire and rapidly heated at a rate of 3.5 × 10^5 K/s, with oxygen evolution monitored by a mass spectrometer.[7,19,20] These results show that the oxide alone can release O_2 at slightly lower temperatures than the ignition temperature for the thermite. Further, a significant amount of gaseous oxygen was present in the system during the Al/CuO reaction. Thus, any condensed phase interaction between the two materials must involve the CuO reduced phase.

The mass spectrometry study showed that violent reaction was possible despite loss of oxygen from the oxygen carrier to the vacuum environment (the O_2 signal). This result is supported by energetic calculations for this system. It requires 265 kJ to heat 2 Al and 3 CuO moles of reactant (which forms 1 mol of Al_2O_3) from room temperature to 1300 K, the temperature at which Al nanoparticles sinter and molten Al escapes the oxide shell and well above the ignition point of Al−CuO.[21] The heat of reaction for that same amount of material is −1208 kJ, which means only ~22% of the reaction enthalpy is required to heat a neighboring reactant of equal volume to the ignition temperature and promote the propagation of the reaction. Even if we suppose that reduction of CuO to Cu_2O is a prerequisite to ignition, then only 38% of the total energy is necessary. Figure 5 provides a schematic diagram of the energy released during these reactions. Therefore, a reaction involving diminished amounts of oxygen may play a large role in the overall propagation of the reaction, with further oxidation occurring heterogeneously with oxygen released from the earlier reduction of CuO.[9]

Another indication that the DTEM experiments are representative of bulk reaction processes is the similarity in morphologies observed under these very different conditions. Figure 6 shows quenched (~300 μs) reaction products from Al/CuO nanothermite mixture ignited on the Pt wire in air. These products, which represents the majority of product volume, exhibits the same characteristic phase-separation found in the product phases of the DTEM experiments, with the two phases existing as adjoining spheres as in Figure 3. In this case, due to the large quantities of material, considerable coalescence results in much larger particles.

From the above considerations, it is reasonable to apply the times scales observed in the DTEM experiment to bulk combustion processes. Al−NPs burn on time scales of 100 μs

DOI: 10.1021/jp5084746
J. Phys. Chem. C 2015, 119, 2792−2797

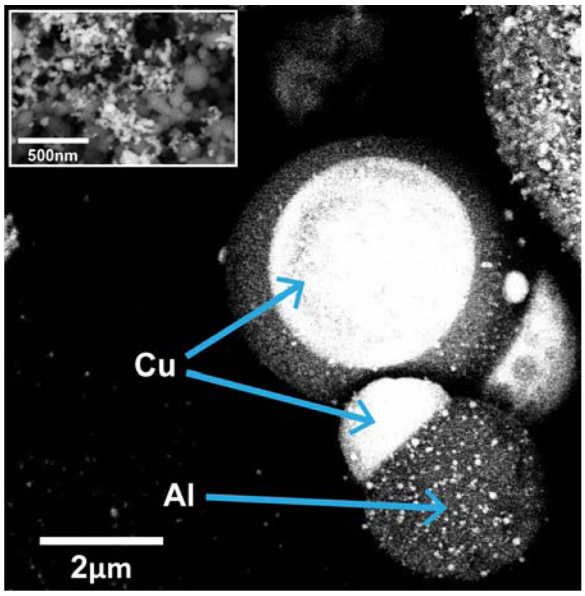

Figure 6. Products of Al/CuO *T*-jump wire ignited combustion that was quenched with a reaction time of ~300 μs. The image was taken with backscattered electrons (BSE) in an SEM, which show denser material as brighter. Thus, the bright phases are copper rich while the darker ones are Al rich. The inset image was also taken with BSE and contains the reactant prior to ignition, which shows the nanoscale nature of the reactant that was lost during reaction. More details of the experimental procedure can be found in another publication.[11]

and longer in pressurized, oxidizing environments.[27,28] Thus, the observed time scales of 0.5−5 μs for reaction indicate that condensed phase reaction mechanisms are much faster than heterogeneous gas-condensed reaction, suggesting that they may play a dominant role in the rapid propagation of the reaction during combustion. Indeed, during constant volume combustion of Al/CuO nanothermite in pressure cells, pressures reach their peak in ~10 μs, which is consistent with the time scales reported here.[29] Further, none of the DTEM experiments contained any evidence of spallation of the metal fuel which would be indicative of the melt dispersion mechanism.[5,12,13] Therefore, a condensed phase "reactive sintering" process is likely.[9]

To apply these DTEM results in a broader manner, a characteristic diffusivity for reaction can be extracted. From the elemental analysis, the oxygen is seen to be homogeneously dispersed throughout the Al region. Therefore, to estimate diffusivity we treat the Al as an oxygen sink in a one-dimensional system with an initial uniform concentration using the following expression:

$$t = \frac{(1.5l)^2}{D}$$

where t is the time scale of depletion, l is the length of region, and D is the characteristic diffusivity.[26] With the characteristic time scales and diffusion lengths corresponding to the DTEM experiments, the average D is ~5×10^{-4} cm^2/s. This value is much higher than those typically discussed for thermite reactions, but compares well to the time scales required to diffuse O in molten Cu at temperatures of ~3000 K, as is expected for reaction of these materials.[29]

In the preceding discussion, we have only considered the length scales related to the size of the aggregate. However, the aggregate size is not well-defined nor a defining quantity for bulk combustion where the materials exist as a millimeter sized powder compact. In this case, the extent of mixing in the powder components controls the kinetics of condensed phase reaction. Indeed, that is also the case for the DTEM results as the larger aggregates studied also had larger areas of segregation. This effect can be seen by comparing Figures 1 and 2. Figure 2 is defined by a ~1000 nm long section of Al in its center, while the regions in Figure 1 are only about 300 nm. Bulk combustion studies have shown that mixing has a huge effect on the performance of these nanothermites, which further supports the importance of the condensed phase interaction.[30]

CONCLUSION

In this study, we have directly observed the morphological changes that occur upon heating of Al/CuO nanothermites with in situ dynamic TEM. We observed the creation of phase-separated adjoining spheroids on the order of ~0.5−5 μs, a large temporal range observed to depend on the aggregate size. A partial reduction of CuO leading to a melt state occurred prior to significant reaction and morphological change. It was found that significant interaction between the two materials occurred, including reaction and alloying. While some of the original oxygen content was lost to the environment, the total energy of this system was such that even ~$^1/_3$ of the heat of reaction may have a significant impact on propagation. The products and overall process of the reaction were found to be comparable with the reaction of bulk phase material. Al NPs burned at faster rates in the DTEM experiments than in gaseous oxidizers, suggesting that the condensed phase reaction may be the dominant mechanism in bulk propagation rather than heterogeneous gas-condensed reaction or melt dispersion.

ASSOCIATED CONTENT

Supporting Information

Images from the work involving CuO alone. This material is available free of charge via the Internet at http://pubs.acs.org.

AUTHOR INFORMATION

Corresponding Author

*(M.R.Z.) E-mail: mrz@umd.edu.

Present Address

§Integrated Dynamic Electron Solutions, Pleasanton, CA 94588, United States

Notes

The authors declare no competing financial interest.

ACKNOWLEDGMENTS

Work conducted by M.R.Z and G.C.E has been supported by the Army Research Office and the Defense Threat Reduction Agency. DTEM Research was supported by the U.S. Department of Energy (DOE), Office of Science, Basic Energy Sciences (BES), under FWP# SCW0979, and the work conducted at LLNL was performed under the auspices of the U.S. Department of Energy by Lawrence Livermore National Laboratory under Contract DE-AC52-07NA27344. We acknowledge the support of the Maryland NanoCenter and its NispLab.

DOI: 10.1021/jp5084746
J. Phys. Chem. C 2015, 119, 2792−2797

REFERENCES

(1) Dreizin, E. L. Metal-Based Reactive Nanomaterials. *Prog. Energy Combust. Sci.* **2009**, *35*, 141−167.

(2) Rogachev, A. S.; Mukasyan, A. S. Combustion of Heterogeneous Nanostructural Systems (Review). *Combust. Explos. Shock Waves* **2010**, *46*, 243−266.

(3) Asay, B. W.; Son, S. E.; Busse, J. R.; Oschwald, D. M. Ignition Characteristics of Metastable Intermolecular Composites. *Propellants, Explos., Pyrotech.* **2004**, *29*, 216−219.

(4) Dean, S. W.; Pantoya, M. L.; Gash, A. E.; Stacy, S. C.; Hope-Weeks, L. J. Enhanced Convective Heat Transfer in Nongas Generating Nanoparticle Thermites. *J. Heat Transfer* **2010**, *132*, 111201.

(5) Sanders, V. E.; Asay, B. W.; Foley, T. J.; Tappan, B. C.; Pacheco, A. N.; Son, S. F. Reaction Propagation of Four Nanoscale Energetic Composites (Al/MoO_3, Al/WO_3, Al/CuO, and Bi_2O_3). *J. Propul. Power* **2007**, *23*, 707−714.

(6) Sullivan, K. T.; Kuntz, J. D.; Gash, A. E. Electrophoretic Deposition and Mechanistic Studies Of Nano-Al/Cuo Thermites. *J. Appl. Phys.* **2012**, *112*, 024316.

(7) Zhou, L.; Piekiel, N.; Chowdhury, S.; Zachariah, M. R. Time-Resolved Mass Spectrometry of the Exothermic Reaction Between Nanoaluminum and Metal Oxides: The Role of Oxygen Release. *J. Phys. Chem. C* **2010**, *114*, 14269−14275.

(8) Martirosyan, K. S.; Zyskin, M. Reactive Self-Heating Model of Aluminum Spherical Nanoparticles. *Appl. Phys. Lett.* **2013**, *102*, 053112.

(9) Sullivan, K. T.; Piekiel, N. W.; Wu, C.; Chowdhury, S.; Kelly, S. T.; Hufnagel, T. C.; Fezzaa, K.; Zachariah, M. R. Reactive Sintering: An Important Component in The Combustion of Nanocomposite Thermites. *Combust. Flame* **2012**, *159*, 2−15.

(10) Piekiel, N. W.; Zhou, L.; Sullivan, K. T.; Chowdhury, S.; Egan, G. C.; Zachariah, M. R. Initiation and Reaction in Al/Bi2O3 Nanothermites: Evidence for the Predominance of Condensed Phase Chemistry. *Combust. Sci. Technol.* **2014**, *186*, 1209−1224.

(11) Jacob, R. J.; Jian, G.; Guerieri, P. M.; Zachariah, M. R. Energy Release Pathways in Nanothermites Follow Through the Condensed Phase. *Combust. Flame* **2014**, *162*, 258−264.

(12) Levitas, V. I.; Asay, B. W.; Son, S. F.; Pantoya, M. Melt Dispersion Mechanism for Fast Reaction of Nanothermites. *Appl. Phys. Lett.* **2006**, *89*, 071909.

(13) Levitas, V. I.; Pantoya, M. L.; Dikici, B. Melt Dispersion versus Diffusive Oxidation Mechanism for Aluminum Nanoparticles: Critical Experiments and Controlling Parameters. *Appl. Phys. Lett.* **2008**, *92*, 011921.

(14) Chowdhury, S.; Sullivan, K.; Piekiel, N.; Zhou, L.; Zachariah, M. R. Diffusive vs Explosive Reaction at the Nanoscale. *J. Phys. Chem. C* **2010**, *114*, 9191−9195.

(15) LaGrange, T.; Campbell, G. H.; Reed, B.; Taheri, M.; Pesavento, J. B.; Kim, J. S.; Browning, N. D. Nanosecond Time-Resolved Investigations Using the in situ of Dynamic Transmission Electron Microscope (DTEM). *Ultramicroscopy* **2008**, *108*, 1441−1449.

(16) LaGrange, T.; Reed, B. W.; Santala, M. K.; McKeown, J. T.; Kulovits, A.; Wiezorek, J. M. K.; Nikolova, L.; Rosei, F.; Siwick, B. J.; Campbell, G. H. Approaches for Ultrafast Imaging of Transient Materials Processes in the Transmission Electron Microscope. *Micron* **2012**, *43*, 1108−1120.

(17) Reed, B. W.; Armstrong, M. R.; Browning, N. D.; Campbell, G. H.; Evans, J. E.; LaGrange, T.; Masiel, D. J. The Evolution of Ultrafast Electron Microscope Instrumentation. *Microsc. Microanal.* **2009**, *15*, 272−281.

(18) Santala, M. K.; Reed, B. W.; Topuria, T.; Raoux, S.; Meister, S.; Cui, Y.; LaGrange, T.; Campbell, G. H.; Browning, N. D. Nanosecond in situ Transmission Electron Microscope Studies of the Reversible $Ge_2Sb_2Te_5$ Crystalline ⇔ Amorphous Phase Transformation. *J. Appl. Phys.* **2012**, *111*, 024309.

(19) Jian, G.; Zhou, L.; Piekiel, N. W.; Zachariah, M. R. Low Effective Activation Energies for Oxygen Release from Metal Oxides: Evidence for Mass-Transfer Limits at High Heating Rates. *ChemPhysChem* **2014**, *15*, 1666−1672.

(20) Jian, G.; Piekiel, N. W.; Zachariah, M. R. Time-Resolved Mass Spectrometry of Nano-Al and Nano-Al/CuO Thermite under Rapid Heating: A Mechanistic Study. *J. Phys. Chem. C* **2012**, *116*, 26881−26887.

(21) Egan, G. C.; Sullivan, K. T.; LaGrange, T.; Reed, B. W.; Zachariah, M. R. In situ Imaging of Ultra-Fast Loss of Nanostructure in Nanoparticle Aggregates. *J. Appl. Phys.* **2014**, *115*, 084903.

(22) Laven, P. MiePlot: a computer program for scattering of light from a sphere using Mie theory & the Debye series, v4.3; 2006.

(23) Polyanskiy, M. N. Refractive index database. http://refractiveindex.info (accessed May 12).

(24) Kosenko, A. V.; Emel'chenko, G. A. Equilibrium Phase Relationships in the System Cu-O under High Oxygen Pressure. *J. Phase Equilib.* **2001**, *22*, 12−19.

(25) Li, J.; Wang, S. Q.; Mayer, J. W.; Tu, K. N. Oxygen-Diffusion-Induced Phase Boundary Migration in Copper Oxide Thin Films. *Phys. Rev. B* **1989**, *39*, 12367−12370.

(26) Kingery, W. D.; Bowen, H. K.; Uhlmann, D. R. *Introduction to Ceramics*; Wiley: New York, 1976.

(27) Huang, Y.; Risha, G. A.; Yang, V.; Yetter, R. A. Combustion of Bimodal Nano/Micron-Sized Aluminum Particle Dust in Air. *Proc. Combust. Inst.* **2007**, *31*, 2001−2009.

(28) Lynch, P.; Krier, H.; Glumac, N. A Correlation for Burn Time of Aluminum Particles in the Transition Regime. *Proc. Combust. Inst.* **2009**, *32*, 1887−1893.

(29) Sullivan, K.; Zachariah, M. R. Simultaneous Pressure and Optical Measurements of Nanoaluminum Thermites: Investigating the Reaction Mechanism. *J. Propul. Power* **2010**, *26*, 467−472.

(30) Nellums, R. R.; Terry, B. C.; Tappan, B. C.; Son, S. F.; Groven, L. J. Effect of Solids Loading on Resonant Mixed Al-Bi2O3 Nanothermite Powders. *Propellants, Explos., Pyrotech.* **2013**, *38*, 605−610.

DOI: 10.1021/jp5084746
J. Phys. Chem. C 2015, 119, 2792−2797